

ADPglucose pyrophosphorylase's N-terminus: Structural role in allosteric regulation

C.M. Bejar^a, M.A. Ballicora^{a,b}, A.A. Iglesias^c, J. Preiss^{a,*}

^a Department of Biochemistry and Molecular Biology, Michigan State University, East Lansing, MI 48824, USA

^b Department of Chemistry, Loyola University Chicago, Chicago, IL 60626, USA

^c Laboratorio de Enzimología Molecular, Facultad de Bioquímica y Ciencias Biológicas, Universidad Nacional del Litoral, Paraje "El Pozo," CC 242, S3000ZAA Santa Fe, Argentina

Received 26 January 2006

Available online 2 March 2006

Abstract

We studied the functional role of the *Escherichia coli* ADPglucose pyrophosphorylase's N-terminus in allosteric regulation, and the particular effects caused by its length. Small truncated mutants were designed, and those lacking up to 15-residues were active and highly purified for further kinetic analyses. NΔ3 and NΔ7 did not change the kinetic parameters with respect to the wild-type. NΔ11 and NΔ15 enzymes were insensitive to allosteric regulation and highly active in the absence of the activator. Co-expression of two polypeptides corresponding to the N- and C-termini generated an enzyme with activation properties lower than those of the wild-type [C.M. Bejar, M.A. Ballicora, D.F. Gómez Casati, A.A. Iglesias, J. Preiss, The ADPglucose pyrophosphorylase from *Escherichia coli* comprises two tightly bound distinct domains, FEBS Lett. 573 (2004) 99–104]. Here, we characterized a NΔ15 co-expression mutant, in which the allosteric regulation was restored to wild-type levels. Unusual allosteric effects caused by either an N-terminal truncation or co-expression of individual domains may respond to structural changes favoring an up-regulated or a down-regulated conformation rather than specific activator or inhibitor sites' disruption.

© 2006 Elsevier Inc. All rights reserved.

Keywords: Glycogen synthesis; ADPglucose pyrophosphorylase; Allosteric regulation; N-terminus deletion

ADPglucose pyrophosphorylase (EC 2.7.7.27; ADPGlc PPase) catalyzes the reaction: $ATP + Glc1P \rightleftharpoons ADPGlc + PP_i$, in the presence of a divalent cation (physiologically Mg^{2+}). Although reversible in vitro, the reaction occurs mainly in the direction of ADPGlc production in vivo, actually being this the limiting step in the pathway of glycogen and starch synthesis in bacteria and plants, respectively [1–3]. ADPGlc PPase is a regulatory enzyme, and the activity is allosterically modulated by key intermediates of the major carbon assimilatory route in the different organisms. Its characterization from many sources allowed for establishing distinctive structural

and regulatory properties for this protein. For example, the enzyme from *Escherichia coli* is a homotetramer (subunit molecular mass around 50 kDa) mainly activated by fructose-1,6-bis-phosphate (FBP) and inhibited by AMP; whereas that found in plants is a ~200 kDa heterotetramer ($\alpha_2\beta_2$) activated by 3P-glycerate and inhibited by inorganic orthophosphate [1–3]. On the basis of their different regulatory properties and considering their biological origin as well as structural characteristics, ADPGlc PPases were grouped in nine different classes [2,3].

The relevance of starch as a natural polymer and raw material for food and non-food industries makes ADPGlc PPase a protein with particular interest in biotechnology [1]. It has been clearly established that manipulation of the starch content in plants requires to manage levels of activity of the enzyme within plastids

* Corresponding author. Fax: +1 517 353 9334.

E-mail address: preiss@msu.edu (J. Preiss).

in specific tissues [1,4]. For these technological purposes, the understanding of the enzyme's regulatory mechanisms is a key issue.

Characterization of amino acids involved in binding of activator for the ADPGlc PPase from *E. coli* and *Agrobacterium tumefaciens* performed by chemical modification and site-directed mutagenesis allowed for pointing out the relevance of the protein's N-terminus (N-t) in allosteric regulation [5–8]. More recent studies performed with chimeric enzymes from these bacteria have indicated the involvement of the N-t together with the C-terminus (C-t) domain (and the interaction between them) in determining the specificity and affinity for the activator [9]. Also, the role of the C-t domain in regulation and its tight interaction with the catalytic region of the protein have been evidenced for the *E. coli* enzyme [10].

The importance of the N-terminal region for the allosteric activation and inhibition of the *E. coli* ADPGlc PPase was evidenced by characterization of truncated enzymes [11,12]. The enzyme lacking 10 to 13 amino acids from the N-t and 2 amino acids from the C-t after treatment with proteinase K is almost independent of the need of FBP for maximal activity and is insensitive to inhibition by AMP [12]. These results were confirmed by engineering a recombinant truncated enzyme with 11 amino acids deleted from the N-t and 2 from the C-t [11]. The unusual regulatory properties of this truncated ADPGlc PPase justified a more detailed characterization of the actual role the N-t extension has in enzyme activation and its interaction with the C-t of the protein. We aimed to analyze here the structural bases determining the enzyme regulatory properties and how the length of the N-t affects the protein ability to arrange specific 3D conformations. We also addressed the question of how the N-t communicates with other domains involved in regulation. As a result, the present work provides us with a more complete understanding of the relationship between structure, function, and regulation of the ADPGlc PPases.

Materials and methods

Construction of N-terminal truncated enzymes

Escherichia coli N-terminal truncated forms (EcNΔ3, EcNΔ7, EcNΔ11, EcNΔ15, EcNΔ19, and EcNΔ22) were encoded by pETEC [9] derivatives and were obtained using the following forward primers, which introduced an *NdeI* site (in *italics*):

EcNΔ3: 5' ATG GTT *CAT ATG* GAG AAG AAC GAT CAC T 3'
 EcNΔ7: 5' GAG AAG *CAT ATG* CAC TTA ATG TTG GCG C 3'
 EcNΔ11: 5' CAC TTA *CAT ATG* GCG CGC CAG CTG CCA 3'
 EcNΔ15: 5' GCG CGC *CAT ATG* CCA TTG AAA TCT GTT 3'
 EcNΔ19: 5' CCA TTG *CAT ATG* GTT GCC CTG ATA CTG G 3'
 EcNΔ22: 5' TCT GTT *CAT ATG* ATA CTG GCG GGA GGA C 3'

The T7 terminator was used as reverse primer. The fragments were sub-cloned in pET24a vector between *NdeI*–*SacI* sites to form pETEC-NΔ3, pETEC-NΔ7, pETEC-NΔ11, pETEC-NΔ15, pETEC-NΔ19, and pETEC-NΔ22.

EcNΔ15-CΔ108 coding DNA was amplified by PCR from pETEC-NΔ15 with the downstream primer used to construct EcCΔ108 [10], which introduced a *SacI* site right after the codon corresponding to amino acid 323. The amplified coding region was then cloned as *NdeI*–*SacI* fragment in pMAB5. The plasmid coding for *E. coli* ADPGlc PPase C-terminal residues 328–431, pMAB6-Ec_{328–431}, was previously obtained [10]. All constructs were verified by DNA sequencing. The constructs used here are schematically shown in Fig. 1.

Expression of the recombinant enzymes

N-terminal truncated enzymes encoded by pETEC derivative vectors, were expressed in *E. coli* BL21(DE3) cells as previously described [9]. EcNΔ15-CΔ108 + Ec_{328–431} were co-expressed in an ADPGlc PPase deficient-*E. coli* B strain, AC70R1-504 [13], as described for EcCΔ108 + Ec_{328–431} [10]. In small-scale expression assays, single colonies of the pETEC-derivatives transformants were grown in 50 ml Luria broth medium at 37 °C with 50 μg/ml kanamycin up to OD₆₀₀ = 0.8. The expression was induced at room temperature (23–25 °C) for 4 h by addition of 1 mM final concentration of IPTG. For the co-expression of the pMAB-derivative plasmids, cells were grown in the same conditions but adding 50 μg/ml kanamycin plus 70 μg/ml spectinomycin and carrying out induction with 1 mM final concentration of IPTG and 5 μg/ml nalidixic acid for 16 h. In both cases, after induction, cells were chilled on ice and harvested by centrifugation. Cell pastes were resuspended in 3 ml buffer A (50 mM Hepes, pH 8.0, 5 mM MgCl₂, 0.1 mM EDTA, and 10% w/v

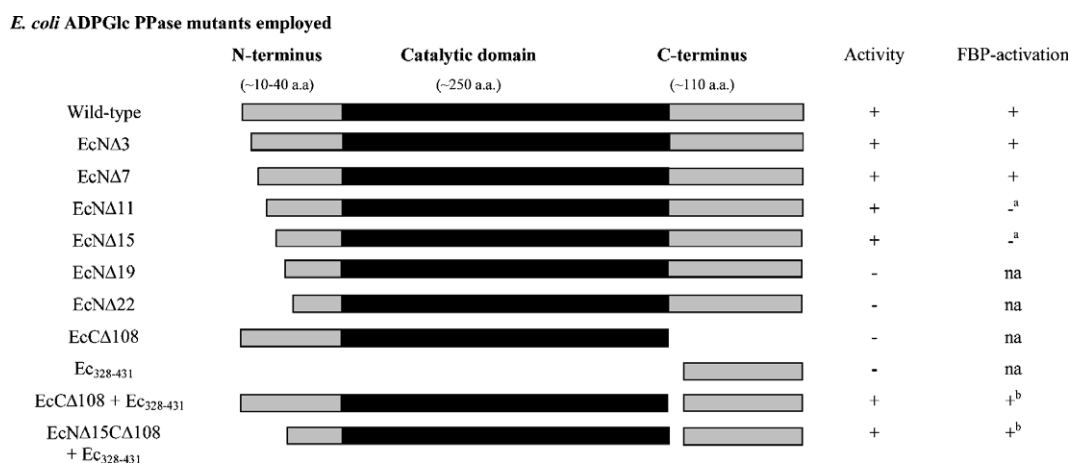


Fig. 1. Summary of *E. coli* ADPGlc PPase constructs studied and their activation properties. (a) The mutant enzymes were fully active in the absence or at low concentration of the activator FBP. (b) Affinity for the activator was lower than the wild-type enzyme. na, non-applicable.

sucrose). All subsequent protein purification steps were conducted at 0–4 °C. Cells were disrupted by sonication, centrifuged for 15 min at 15,000g, and the supernatants (crude extracts) were stored at –80 °C. Dilutions of the samples (2-fold and 10-fold) were tested for activity in the pyrophosphorolysis direction as described below.

Purification of N-truncated ADPGlc pyrophosphorylase mutants

Recombinant *E. coli* BL21(DE3) were grown in 1–2 L and induced as described above. The cell pastes were resuspended in 15–30 ml of buffer A, sonicated, and the lysates were cleared by centrifugation. The resulting crude extracts were applied to a DEAE-Fractogel column (EMD Chemicals Inc) and eluted with a linear NaCl gradient (0–0.5 M). The active fractions were pooled and precipitated with a 30–60% ammonium sulfate cut. After centrifugation, the pellet was resuspended in buffer A and desalted on Bio-Rad 10 DG chromatography columns equilibrated with the same buffer. The desalted samples were individually applied to a Mono Q HR 10/10 (FPLC, Pharmacia) column, equilibrated with buffer A, and eluted with a linear NaCl gradient (0–0.5 M). The purest fractions (as assessed by SDS–PAGE) were pooled and concentrated using Centricon-30 devices (Amicon Inc.). After this step, EcNΔ3, EcNΔ7, and EcNΔ15 were >95% pure. EcNΔ11 MonoQ active fractions were pooled, concentrated by 80% ammonium sulfate precipitation, applied to a phenyl–Superose (FPLC, Pharmacia) column, and eluted with a decreasing gradient of ammonium sulfate (1.2–0.0 M). The active fractions were pooled and concentrated with Centricon-30 devices.

Purification of co-expressed EcNΔ15-CA108 + Ec_{328–431}

Over-expression and purification were carried out as described for EcCA108 + Ec_{328–431} [10].

Protein assay

Protein concentration in the crude extracts and in the subsequent purification steps was measured using the bicinchoninic acid reagent [14] (Pierce Chemical Co.), with BSA as the standard. Protein concentration of the purified enzymes was determined by UV absorbance at 280 nm using an extinction coefficient of 1.0 ml mg⁻¹ cm⁻¹ [15].

Protein electrophoresis and immunoblotting

Purification of the recombinant proteins was monitored by SDS–PAGE as described by Laemmli [16], using 4–15% Tris–HCl pre-cast gradient polyacrylamide gels (Bio-Rad). Perfect™ protein markers were used as molecular mass standards. Following electrophoresis, protein bands were either visualized by staining with Coomassie brilliant blue R-250 or electroblotted onto a Protran™ nitrocellulose membrane. The membrane was then treated with affinity-purified anti-*E. coli* B strain AC70R1 ADPGlc PPase IgG [15]. The resulting antigen–antibody complex was visualized by treatment with alkaline phosphatase-linked goat anti-rabbit IgG and then stained with BM purple AP-substrate precipitating reagent (Roche Molecular Biochemicals).

Enzymatic activity assays

Assay A: pyrophosphorolysis. Formation of [³²P]ATP from [³²P]PP_i in the direction of pyrophosphorolysis at 37 °C was determined by the method previously described [17]. Unless otherwise indicated, the reaction was carried out for 10 min in a mixture that contained 50 mM Hepes (pH 8.0), 7 mM MgCl₂, 1.5 mM [³²P]PP_i (1500–2500 cpm/nmol), 2 mM ADPGlc, 2 mM FBP, 4 mM NaF, and 0.05 mg/ml BSA, plus enzyme in a total volume of 250 μl.

Assay B: synthesis. Formation of [¹⁴C]ADPglucose from [¹⁴C]Glc1P in the synthesis direction was determined at 37 °C by the method of Yep and co-workers [18]. The reaction was carried out for 10 min in a mixture

containing 50 mM HEPES (pH 8.0), 7 mM MgCl₂, 0.5 mM [¹⁴C]Glc1P (~1000 dpm/nmol), 1.5 mM ATP, 2 mM FBP, 0.0015 U/μl pyrophosphatase, and 0.2 mg/ml BSA, plus enzyme in a total volume of 200 μl.

One unit of enzymatic activity is equal to 1 μmol of product, either [³²P]ATP or [¹⁴C]ADPGlc, formed per min at 37 °C.

Kinetic characterization

Kinetic data were plotted as specific activity (nmol min⁻¹ mg⁻¹) versus substrate or effector concentration. Kinetic constants were acquired by fitting the data to the Hill equation with a non-linear least-squares formula using the program Origin™ 5.0. Hill plots were used to calculate the Hill coefficient *n*_H and the kinetic constants that correspond to the activator, substrate or inhibitor concentrations giving 50% of the maximal activation (*A*_{0.5}), velocity (*S*_{0.5}), and inhibition (*I*_{0.5}).

Results and discussion

Purification and characterization of *E. coli* ADPGlc PPase N-terminal truncated forms

To evaluate in detail the structural role of the N-t extension in allosteric regulation, small deletion mutants of the ADPGlc PPase from *E. coli* were designed (Fig. 1) and tested. EcNΔ3, EcNΔ7, EcNΔ11, EcNΔ15, EcNΔ19, and EcNΔ22 truncated proteins were over-expressed in *E. coli* BL-21 and purified in small-scale. EcNΔ3, EcNΔ7, and EcNΔ15 were enriched to >95% and EcNΔ11 to 60–70% purity (Table 1). As shown in Table 1, the four mutants had specific activities comparable to that of the purified wild-type enzyme. Thus, the N-t comprising at least 15 amino acid residues of the *E. coli* ADPGlc PPase is not essential for catalytic activity. Conversely, deletions of 19- and 22-residues from the N-t significantly decreased the activity of ADPGlc PPase in the crude extracts. In fact, enzymatic activity of EcNΔ19 measured by the pyrophosphorolysis assay was two orders of magnitude lower than that of the wild-type (also in the crude extract), whereas the activity of EcNΔ22 was negligible (Table 1).

Table 1
Specific activities of wild-type and N-terminal truncated *E. coli* ADPGlc PPases

Sample	Specific activity (U/mg)	Purity (%)	FBP-activation kinetics		Activation-fold
			<i>A</i> _{0.5} (μM)	<i>n</i> _H	
Ec wild-type	131	90	36.4 ± 1.7	2.1	29.5
EcNΔ3	94	>95	52.3 ± 5.6	1.8	23.5
EcNΔ7	65	>95	88.7 ± 3.9	2.9	22.0
EcNΔ11	98	60–70	—	—	1.0
EcNΔ15	105	>95	—	—	1.2
Ec wild-type ^a	24	20–30	—	—	—
EcNΔ19 ^b	0.5	15–20	—	—	—
EcNΔ22 ^b	<0.005	15–20	—	—	—

Specific activities and FBP-activation kinetics were determined by the pyrophosphorolysis assay. Purity of the samples was estimated from SDS–PAGE gels.

^a Determined in crude extracts [9].

^b Determination in crude extracts.

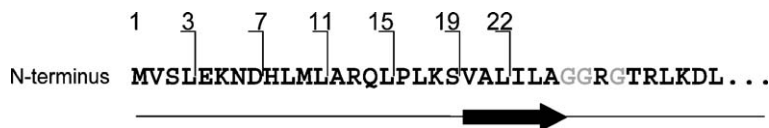


Fig. 2. N-terminal *E. coli* ADPGlc PPase sequence and predicted secondary structures. Residues 1 to 18 are predicted to be a loop. Ser¹⁹ is predicted to be at the N-terminal end of a β strand in which Leu²² resides. The Gly-rich loop (in grey) is similar to P-loop-like motif present in protein kinases and nucleotide-binding sites.

Results shown in Table 1 were consistent with the predicted secondary structures of ADPGlc PPase [19] and with the 3D model previously proposed [2]. This model was also validated with the data derived from the crystal structure of an inhibited form of the homotetrameric (small subunit) enzyme from potato tuber [20]. In the structural model, the N-terminal tail is a loop preceding a β strand starting at Ser¹⁹ (Fig. 2). Following that, β strand is a glycine-rich loop similar to the P-loop motif present in protein kinases and nucleotide-binding sites. The 19- and 22-residue N-terminal deletions may cause destabilization of the local secondary structure (including the glycine-rich loop) that propagates to other important regions in the overall protein structure. Kinetic analysis of EcN Δ 3, EcN Δ 7, EcN Δ 11, and EcN Δ 15 showed that removal of up to 7-residues from the N-terminus does not significantly alter the FBP-activation properties of the enzyme. EcN Δ 3 and EcN Δ 7 mutants behaved in ways similar to the wild-type enzyme, which is activated 20- to 30-fold by the specific effector (Fig. 3 and Table 1). On the other hand, EcN Δ 11 behaved as reported previously [11,12] and as EcN Δ 15. Both mutant enzymes were highly active even in the absence of FBP, showing almost no activation (Fig. 3 and Table 1). Additionally, EcN Δ 15 was tested

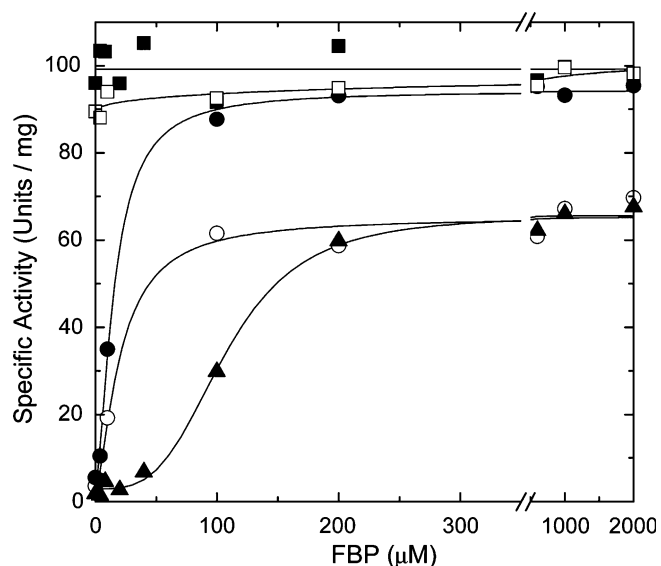


Fig. 3. FBP activation of wild-type and the N-terminal truncated *E. coli* ADPGlc PPases. (○) Wild-type, (●) N Δ 3, (▲) N Δ 7, (■) N Δ 11, and (□) N Δ 15. Saturation plots were determined by the pyrophosphorolysis reaction.

for its ability to be inhibited by AMP (Fig. 4). Because it has been demonstrated that inhibition of the *E. coli* ADPGlc PPase by AMP requires the presence of at least traces of FBP in the medium [21], we performed inhibition kinetics at two different activator concentrations: 30 and 130 μ M (Figs. 4A and B, respectively). A similar lack of sensitivity of EcN Δ 15 for this inhibitor was also exhibited by the EcN Δ 11 mutant [11,12]. Results suggested that deletion of 11- or 15- residues from the N-t induces spatial arrangements favoring a more active conformation of the enzyme and possibly disrupting the AMP site.

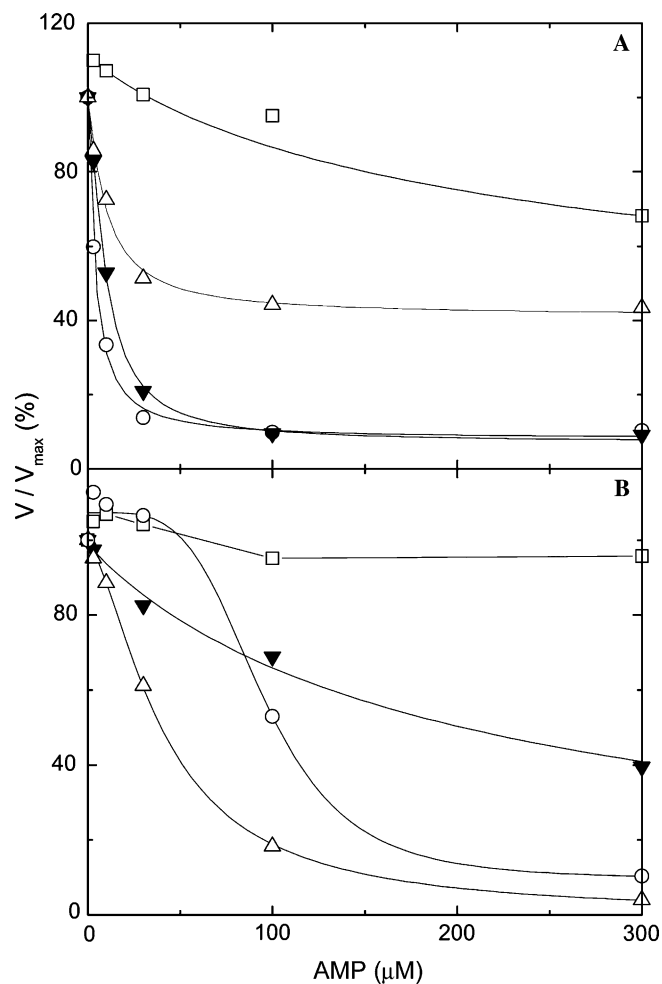


Fig. 4. AMP inhibition kinetics of wild-type and mutants *E. coli* ADPGlc PPases. All determinations were obtained by synthesis assay in the presence of (A) 30 or (B) 130 μ M FBP. (○) Wild-type, (□) N Δ 15, (Δ) EcC Δ 108 + Ec₃₂₈₋₄₃₁, and (▼) EcN Δ 15C Δ 108 + Ec₃₂₈₋₄₃₁.

Characterization of *EcNΔ15-CA108 + Ec_{328–431}*

To evaluate the opposite effects on FBP-activation caused by an N-terminal deletion [11,12] and by a nick separating the catalytic domain and the C-t [10], *EcNΔ15C-Δ108 + Ec_{328–431}* were co-overexpressed and purified as described in Materials and methods. As illustrated in Table 2, after the Green A affinity chromatography the co-expressed proteins were purified to at least 90%. The *EcNΔ15C-Δ108 + Ec_{328–431}* co-expression product showed a specific activity comparable to those of the *EcC-Δ108 + Ec_{328–341}* [10], the *EcNΔ15*, and the wild-type enzymes (Table 2). Two protein bands of the expected molecular sizes (i.e., ~35 kDa and ~12 kDa) were observed in SDS-PAGE and Western blot (data not shown) of purified *EcNΔ15C-Δ108 + Ec_{328–431}*. Interestingly, the kinetic properties of this co-expressed protein were comparable to those of the wild-type enzyme regarding affinity for the substrate ATP, affinity for the activator FBP, and inhibition by AMP (Table 3).

Saturation kinetics for the FBP-activation (Fig. 5) and AMP inhibition (Fig. 4) indicated that the *EcNΔ15C-Δ108 + Ec_{328–431}* co-expressed enzyme recovered the sensitivity for the allosteric effectors that was, respectively, lost or decreased in the *EcNΔ15* or *EcC-Δ108 + Ec_{328–431}* mutant enzymes. Thus, the opposite effects in FBP-activation caused by an N-terminal deletion and by a nick separating the C-t and the catalytic domain seemed to compensate when these structural modifications were com-

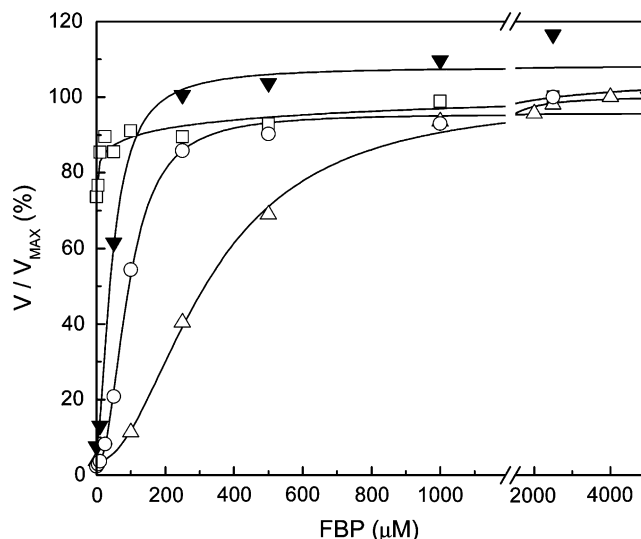


Fig. 5. FBP-activation kinetics of wild-type and mutants *E. coli* ADPGlc PPases. All determinations were obtained by synthesis assay. (○) Wild-type, (□) *NΔ15*, (△) *EcCA108 + Ec_{328–431}*, and (▼) *EcNΔ15C-Δ108 + Ec_{328–431}*.

bined in the same protein. Assuming that an allosteric enzyme in solution is present as a mixture of conformations with different levels of activities, a 15 N-terminal residue truncation may induce the same structural change as the allosteric activator, which drives the equilibrium between enzyme species towards the more active one. In contrast, the structure arrangement generated when the catalytic domain and the C-t are co-expressed as individual polypeptides may favor a less active conformation. Combination of these two modifications in *EcNΔ15-CA108 + Ec_{328–431}* might have compensated their opposite kinetic effects, making this mutant enzyme more similar to the wild-type enzyme. It is noteworthy that this mutant was also sensitive to AMP inhibition, eliminating the above suggestion of a possible AMP site disruption caused by deletion of 15 N-terminal residues. It is more likely that *EcNΔ15* is locked in a more active conformation that cannot be reversed by the inhibitor.

Integration of our biochemical results involving the N-terminal extension with actual structural data remains

Table 2
Specific activities of wild-type and mutants *E. coli* ADPGlc PPases

Sample	Specific activity (U/mg)		Purity (%)
	Pyrophosphorolysis	Synthesis	
Wild-type ^a	131	54	90
<i>EcCA108</i> ^a	<0.001	<0.0001	50–60
<i>EcCA108 + Ec_{328–431}</i> ^a	132	43	>95
<i>EcNΔ15</i>	105	62	>95
<i>EcNΔ15CA108 + Ec_{328–431}</i>	86	30	90

Specific activities were determined in purified samples. Purity of the samples was estimated from SDS-PAGE gels.

^a Data obtained from [10].

Table 3
Kinetic parameters of wild-type and mutants *E. coli* ADPGlc PPases

Enzyme	ATP		FBP activation		AMP inhibition			
	$S_{0.5}$ (μM)	n_H	$A_{0.5}$ (μM)	n_H	30 μM FBP		130 μM FBP	
					$I_{0.5}$ (μM)	n_H	$I_{0.5}$ (μM)	n_H
<i>Ec</i> wild-type ^a	301.1 ± 14.1	1.9	92.1 ± 0.5	2.1	3.8 ± 0.4	1.1	94.0 ± 9.9	2.7
<i>EcCA108 + Ec_{328–431}</i> ^a	1410.2 ± 51.4	2.9	327.4 ± 15.5	2.0	9.7 ± 1.9	1.2	40.7 ± 2.6	1.6
<i>EcNΔ15CA108 + Ec_{328–431}</i>	494.6 ± 33.4	1.6	45.9 ± 8.1	1.6	9.4 ± 0.7	1.6	206 ± 24	0.9
<i>EcNΔ15</i>	nd	nd	6.9 ± 0.6	2.0	ni	—	ni	—

All determinations were obtained by synthesis assay.

nd, not determined.

ni, no inhibition was observed when assayed up to 300 μM concentration of AMP.

^a Data obtained from [10].

to be done since the only ADPGlc PPase crystal structures available lack a solved diffraction pattern corresponding to the first 11 N-terminal amino acids. The structural data point to the flexible character of this region of the enzyme which agrees with its suggested regulatory role as “allosteric switch.” It would be very valuable to obtain direct structural information of all the mutants analyzed in the present work. They would provide with a series of snapshots of the various conformations achieved by the enzyme in the different activated states, allowing for a better understanding of the allosteric regulatory mechanism.

Acknowledgments

This work was supported in part by Department of Energy Research Grant DE-FG 02-93ER20121, Northern Regional USDA Grant NCI-142, and USDA-BARD Grant IS-3733-DSR (to JP); and CAI + D, ANPCyT: PICT'03 1-14733, PICTO'03 1-13241, and PAV'03 137 (to AAI). AAI is a Research Career Member from CONICET (Argentina).

References

- [1] M.N. Sivak, J. Preiss, Starch: basic science to biotechnology, in: S.L. Taylor (Ed.), *Advances In Food and Nutrition Research*, Academic Press, San Diego, 1998, pp. 1–199.
- [2] M.A. Ballicora, A.A. Iglesias, J. Preiss, ADPglucose pyrophosphorylase; a regulatory enzyme for bacterial glycogen synthesis, *Microbiol. Mol. Biol. Rev.* 67 (2003) 213–225.
- [3] M.A. Ballicora, A.A. Iglesias, J. Preiss, ADP-glucose pyrophosphorylase, a regulatory enzyme for plant starch synthesis, *Photosynth. Res.* 79 (2004) 1–24.
- [4] D.M. Stark, K.P. Timmerman, G.F. Barry, J. Preiss, G.M. Kishore, Role of ADPglucose pyrophosphorylase in regulating starch levels in plant tissues, *Science* 258 (1992) 287–292.
- [5] T.F. Parsons, J. Preiss, Biosynthesis of bacterial glycogen. Isolation and characterization of the pyridoxal-P allosteric activator site and the ADP-glucose-protected pyridoxal-P binding site of *Escherichia coli* B ADP-glucose synthase, *J. Biol. Chem.* 253 (1978) 7638–7645.
- [6] T.F. Parsons, J. Preiss, Biosynthesis of bacterial glycogen. Incorporation of pyridoxal phosphate into the allosteric activator site and an ADP-glucose-protected pyridoxal phosphate binding site of *Escherichia coli* B ADP-glucose synthase, *J. Biol. Chem.* 253 (1978) 6197–6202.
- [7] D.F. Gomez-Casati, R.Y. Igarashi, C.N. Berger, M.E. Brandt, A.A. Iglesias, C.R. Meyer, Identification of functionally important amino-terminal arginines of *Agrobacterium tumefaciens* ADP-glucose pyrophosphorylase by alanine scanning mutagenesis, *Biochemistry* 40 (2001) 10169–10178.
- [8] A. Gardiol, J. Preiss, *Escherichia coli* E-39 ADPglucose synthetase has different activation kinetics from the wild-type allosteric enzyme, *Arch. Biochem. Biophys.* 280 (1990) 175–180.
- [9] M.A. Ballicora, J.I. Sesma, A.A. Iglesias, J. Preiss, Characterization of chimeric ADPglucose pyrophosphorylases of *Escherichia coli* and *Agrobacterium tumefaciens*. Importance of the C-terminus on the selectivity for allosteric regulators, *Biochemistry* 41 (2002) 9431–9437.
- [10] C.M. Bejar, M.A. Ballicora, D.F. Gómez Casati, A.A. Iglesias, J. Preiss, The ADP-glucose pyrophosphorylase from *Escherichia coli* comprises two tightly bound distinct domains, *FEBS Lett.* 573 (2004) 99–104.
- [11] M.X. Wu, J. Preiss, Truncated forms of the recombinant *Escherichia coli* ADP-glucose pyrophosphorylase: the importance of the N-terminal region for allosteric activation and inhibition, *Arch. Biochem. Biophys.* 389 (2001) 159–165.
- [12] M.X. Wu, J. Preiss, The N-terminal region is important for the allosteric activation and inhibition of the *Escherichia coli* ADP-glucose pyrophosphorylase, *Arch. Biochem. Biophys.* 358 (1998) 182–188.
- [13] A.A. Iglesias, G.F. Barry, C. Meyer, L. Bloksberg, P.A. Nakata, T. Greene, M.J. Laughlin, T.W. Okita, G.M. Kishore, J. Preiss, Expression of the potato tuber ADP-glucose pyrophosphorylase in *Escherichia coli*, *J. Biol. Chem.* 268 (1993) 1081–1086.
- [14] P.K. Smith, R.I. Krohn, G.T. Hermanson, A.K. Mallia, F.H. Gartner, M.D. Provenzano, E.K. Fujimoto, N.M. Goeke, B.J. Olson, D.C. Klenk, Measurement of protein using bicinchoninic acid, *Anal. Biochem.* 150 (1985) 76–85.
- [15] T.H. Haugen, A. Ishaque, J. Preiss, Biosynthesis of bacterial glycogen. Characterization of the subunit structure of *Escherichia coli* B glucose-1-phosphate adenyltransferase (EC 2.7.7.27), *J. Biol. Chem.* 251 (1976) 7880–7885.
- [16] U.K. Laemmli, Cleavage of structural proteins during the assembly of the head of bacteriophage T4, *Nature* 227 (1970) 680–685.
- [17] M.K. Morell, M. Bloom, V. Knowles, J. Preiss, Subunit structure of spinach leaf ADPglucose pyrophosphorylase, *Plant Physiol.* 85 (1987) 182–187.
- [18] A. Yep, C.M. Bejar, M.A. Ballicora, J.R. Dubay, A.A. Iglesias, J. Preiss, An assay for adenosine 5'-diphosphate (ADP)-glucose pyrophosphorylase that measures the synthesis of radioactive ADP-glucose with glycogen synthase, *Anal. Biochem.* 324 (2004) 52–59.
- [19] J.B. Frueauf, M.A. Ballicora, J. Preiss, Aspartate residue 142 is important for catalysis by ADP-glucose pyrophosphorylase from *Escherichia coli*, *J. Biol. Chem.* 276 (2001) 46319–46325.
- [20] X. Jin, M.A. Ballicora, J. Preiss, J.H. Geiger, Crystal structure of potato tuber ADP-glucose pyrophosphorylase, *EMBO J.* 24 (2005) 694–704.
- [21] J. Preiss, L. Shen, E. Greenberg, N. Gentner, Biosynthesis of bacterial glycogen. IV. Activation and inhibition of the adenosine diphosphate glucose pyrophosphorylase of *Escherichia coli* B, *Biochemistry* 5 (1966) 1833–1845.